Proceedings of 12th Cambridge Workshop on Cool Stars, Stellar Systems, & The Sun, 2003 University of Colorado.

After the Flare: The Perplexing Spectrum of FK Com

Derek L. Buzasi[1], David P. Huenemoerder[2], Heather L. Preston[1]

Abstract.

FK Com, whose peculiarities were first noted by Merrill (1948), is a single G-type giant rotating near the breakup velocity ($v \sin i$ = 162.5 km s^{-1}; see Huenemoerder *et al.* 1993). The angular momentum derived from this rapid rotation, which corresponds to a period of 2.4 days (Chugainov 1976), exceeds that possible for a main sequence progenitor, and there is no detected orbital motion, so the hypothesis has been advanced that FK Com is in fact a recently coalesced binary (see, *e.g.* Ramsey *et al.* 1981, Huenemoerder *et al.* 1993). FK Com thus provides a unique laboratory in which to study the stellar dynamo under extreme conditions in a single star, independent of interactions due to a binary companion. In this paper, we discuss recent Chandra HETG observations of this unusual object.

1. Observations

We observed FK Com ($m_V = 8.17$) for 40 kiloseconds during March 2000 using the Chandra ACIS-S/HETG. The spectrum (Figure 1) is dominated by lines from highly ionized species of iron, such as Fe XXIV, XXV, and XXVI, indicating the presence of very high-temperature coronal material. Line and continuum intensities were variable during the observation, with the dominant change being a peak followed by a monotonic decay in these intensities, which we interpret as the aftereffects of a flare. Among the interesting features of the spectrum are the fairly large Fe XVII(λ15.265Å)/Fe XVII(λ15.014Å) and Fe XVII($\lambda\lambda$17.051Å + 17.096Å)/Fe XVII(λ15.014Å) ratios, which have been claimed in the case of the solar corona to indicate opacity, and which we discuss in more detail below.

Data were reduced in the usual way for Chandra ACIS-S/HETG observations; the pipeline standard processing occurred using, and event lists were processed with, the CIAO 2.1 (Chandra Interactive Analysis of Observations) software suite. Further analysis products were made with the CIAO tools to filter bad events (based on grade and bad pixels), bin spectra, make light curves, make response functions, and generate spectra — both whole-observation and time-segregated by flare and quiescent ("low-state") states of FK Com – during the 40 ks observation. Analysis of the products from the CIAO tools was performed both with ISIS and with Sherpa, and the fluxes obtained were com-

[1]United States Air Force Academy

[2]Massachusetts Institute of Technology

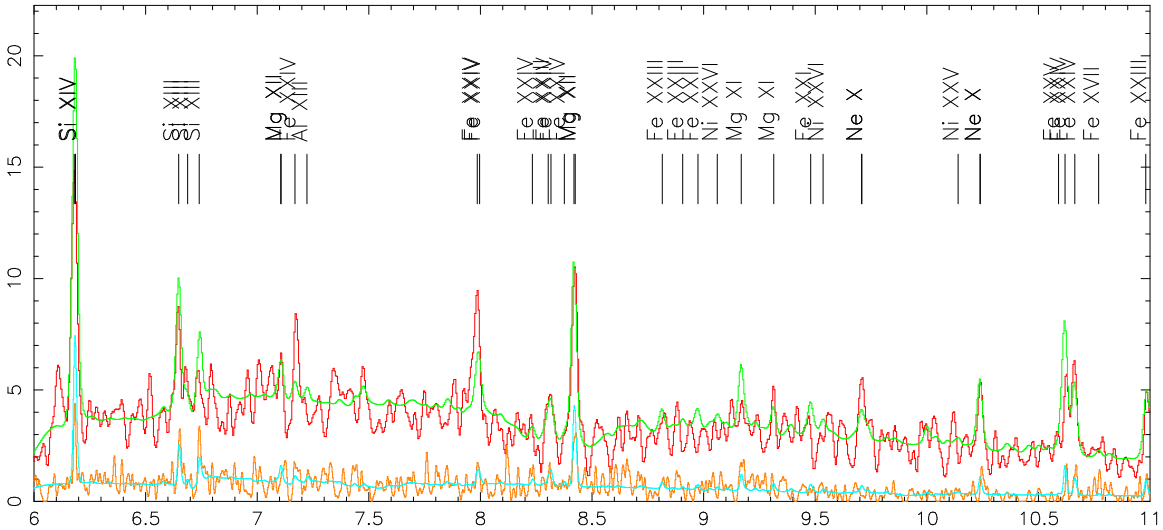

Figure 1. A portion of the Chandra spectrum of FK Com. The wavelength scale is in Å and the vertical axis is in counts. The upper set of curves show the MEG spectrum (black line) and the spectrum resulting from the DEM model shown in Figure 3 (red line), while the lower set of curves show the corresponding result for the HEG spectrum. For display, the spectrum is smoothed by convolution with a Gaussian while for flux determinations the observed spectrum was binned at the instrument resolution and the model spectrum was binned from the APED and folded through the instrumental response function. The strongest lines are labeled.

pared to one another as a consistency check. The DEMs were constructed using APED 1.01 (Astrophysical Plasma Emission Database) in conjunction with the solar abundances of Anders and Grevasse (1989) and the ionization balance of Mazzotta et al. (1998).

Unfortunately, the signal-to-noise ratio was low in many lines which are important for plasma diagnostics, and due to the existence of the flare the situation for modeling is worse: in this paper we present only a DEM (differential emission measure) combined-spectrum model, while with sufficient counts we would normally hope to calculate both a "flare" and a "low-state" model. The signal-to-noise ratio for the combined data is greater than 4 sigma in the strongest lines (λ6.18Å and λ12.14Å).

2. Time Variability

The upper portion of Figure 2 shows the light curve, obtained by binning orders from -3 to +3. It exhibits the quick rise and exponential decay typical of a flare, rising from the start of the observation at 0 ks to peak at 2.5 ks, beginning its decay around 7 ks, and tailing off all the way to 40 ks. The width of the line in each case indicates the uncertainties in the total flux. The small departures

from exponential decay which are visible may be due to rotational modulation, as the relatively cool dense corotating material known to be present around FK Com (Ramsey, Nations, & Barden 1981) obscures the flare site; note that the rotational period of FK Com (207 ks) is several times larger than the flare lifetime.

As expected during a hot flare, the continuum (due predominantly to thermal bremsstrahlung) was obvious during the high state, but disappeared rapidly as the flare progressed. The lower portion of Figure 2 summarizes the behavior of the continuum by showing the time behavior of hardness ratios based on light curves made in short (2−6Å), medium (6−10Å), and long (10−14Å) wavelength bands, which sample the continuum strength at different temperatures.

3. Differential Emission Measure Modeling

Figure 3 shows our DEM fit for the entire observation (flare plus quiescent "low" state). Our DEM model assumes solar abundances. The fit is shown as a solid smooth-filled curve, except above $\log T = 7.9$, where the fit is dependent on a single high-temperature line (Fe "K" line, 1.78Å) and we have therefore cross-hatched the curve to emphasize the greater uncertainty of the model fit. The DEM fit shows a distinct low-state bump from $\log T = 7.2$ to $\log T = 7.7$, superimposed on which appears to be the flare contribution, which rises from $\log T = 7.7$ to peak around $\log T = 8.0$, and for which the peak emission is about four times the maximum quiescent DEM level; compare this with the RS CVn star II Pegasi (Huenemoerder, Canizares, & Schulz 2001) where the flare and bump contributions were similar but at lower temperatures – the bump from 6.8 to 7.6, with the flare component peaking at $\log T = 7.65$. As in the case of FK Com, the flare observed by Huenemoerder, Canizares, & Schulz in II Peg showed peak emission about four times the maximum quiescent DEM. Our observation is thus consistent with the behavior of flares observed in II Peg and other RS CVn stars (see, *e.g.* Huenemoerder *et al.* 2001, Mewe *et al.* 1997, Gudel *et al.* 1999); in particular, the flare adds a discrete high-temperature emission source, and the emission from the cooler source is constant. We also note that the presence of material at temperatures as high as $\log T = 8.0$ tends to confirm earlier reports of the presence of such material, based on ROSAT observations (see, *e.g.* Welty & Ramsey 1994).

4. Resonant Scattering

The theoretical ratio of Fe XVII λ15.265Å/Fe XVII λ15.014Å is 0.25 ± 0.04. The λ15.014Å line has a shorter mean free path than its resonance line neighbor at λ15.265Å, and opacity effects have therefore been suspected in the solar atmosphere, where the observed line ratio is 0.49 ± 0.05 (Saba *et al.* 1999). However, improved laboratory measurements by Brown *et al.* (1998) yielded 0.33 ± 0.01 for this ratio, and Laming *et al.* (2000) measured both this ratio (finding 0.40 ± 0.02) and the ratio of the nearby 17Å pair ($\lambda\lambda 17.051 + 17.096$Å) to the λ15.014Å resonance line which shares the same lower level. For the latter ratio Laming *et al.* found 0.9 ± 0.1 for a beam energy of 125 keV.

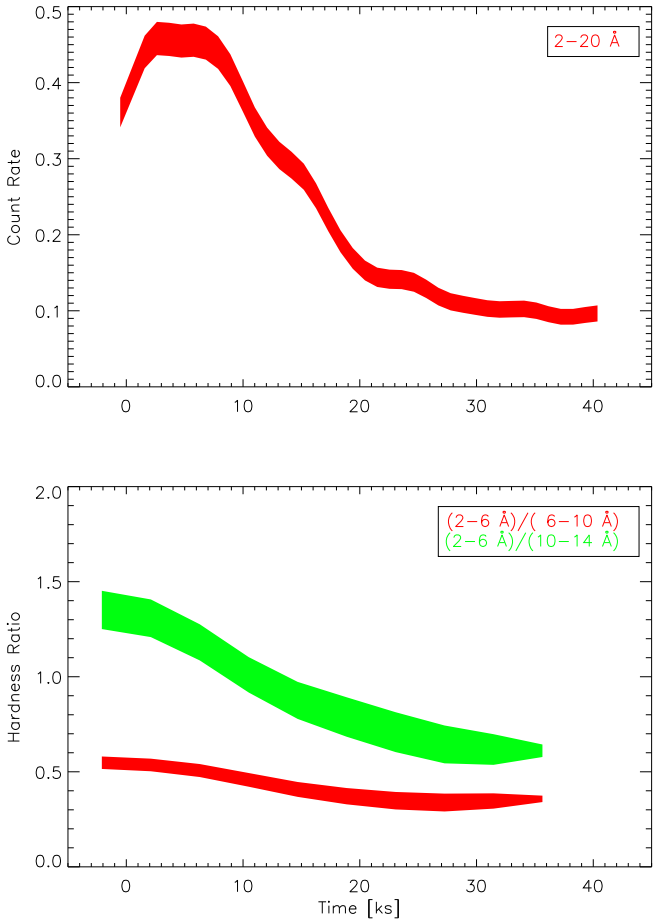

Figure 2. The upper panel shows the light curve resulting from binning events from orders -3 to +3 (omitting the zero order) for both MEG and HEG, from 1.7 to 20Å. The vertical width of both curves is equal to the 1σ uncertainty. The quick rise and exponential decay are typical of a flare. The lower panel shows hardness ratios which indicate the relative strength of the short, medium, and long wavelength continua, and thus should be proxies for temperature. The flux increase was proportionally larger at short wavelengths, thus confirming the high flare temperature. As in the upper panel, the vertical width of the curves is equal to the 1σ uncertainty.

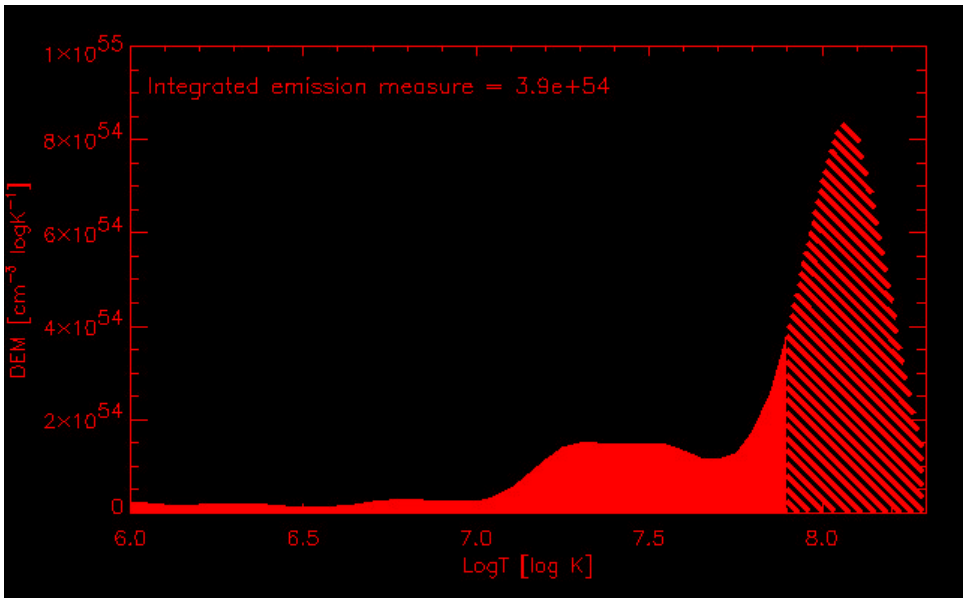

Figure 3. The differential emission measure model for the entire observation of FK Com. The high-temperature portion is cross-hatched to indicate its high uncertainty relative to the lower-temperature portion of the model. The general shape of the distribution – both low- and high-temperature components – is similar to that seen during a flare in II Peg (Huenemoerder *et al.* 2001), but at $\log T = 0.4$ dex higher.

These newer results have led both groups to conclude that observers had been comparing observed ratios to predicted ratios which were too low, and thus that solar opacity effects had been overemphasized. In our data, the ratio of Fe XVII(λ15.265Å)/Fe XVII(λ15.014Å) is 0.77 ± 0.4 and Fe XVII($\lambda\lambda$17.051 + 17.096Å)/Fe XVII(λ15.014Å) is 1.9 ± 0.9. Unfortunately, our signal-to-noise ratio is too low for these measurements to be anything other than suggestive, and while they appear to indicate that in FK Com opacity is a factor in determining the line ratio, they are statistically consistent with the new lab measurements.

We have also examined the ratio of O VIII Lyβ/Lyα, and find that our 3σ upper limit of 0.28 is consistent with the theoretical value of 0.16; the use of an upper limit is caused by the presence of a small forest of Fe lines surrounding O VIII Lyβ, resulting in a large uncertainty in that line's flux despite the strong (better than 3σ) Lyα measurement.

Acknowledgments. DLB and HLP gratefully acknowledge support from the CXC GO award GO0-1080A and from the US Air Force Academy. DPH acknowledges support by SAO contract SV1-61010 (CXC) and GO0-10880B (CXO) to MIT.

References

Anders, E. & Grevasse, N. 1989, Geochimica et Cosmochimica Acta 53, 197

Brown, G.V., Beiersdorfer, P., Liedahl, D.A., *et al.* 1998, ApJ, 502, 1015

Chugainov, P.F. 1976, Izv. Krymsk. Ap. Obs. 54, 89

Gudel, M., Linsky, J.L., Brown, A., & Nagase, F. 1999, ApJ, 511, 405

Huenemoerder, D.P, Ramsey, L.W., Buzasi, D.L., & Nations, H.L. 1993, ApJ, 404, 316

Huenemoerder, D.P., Canizares, C.R., & Schulz, N.S. 2001, ApJ, submitted

Laming, J.M. *et al.* 2000, ApJ, 545, L161

Mazzotta, P., Mazzitelli, G., Colafrancesco, S., & Vittorio, N. 1998, A&A, 133, 403

Merrill, P.W. 1948, PASP, 60, 382

Mewe, R., Kaastra, J.S., van den Oord, G.H.J., Vink, J., & Tawara, Y. 1997, A&A, 320, 147

Ramsey, L.W., Nations, H.L., & Barden, S.C. 1981, ApJ, 251, 101

Saba, J.L.R., Schmelz, J.T., Bhatia, A.K., & Strong, K.T. 1999, ApJ, 510, 1064

Welty, A.D. & Ramsey, L.W. 1994, AJ, 108, 299